https://doi.org/10.31925/farmacia.2023.6.3 **ORIGINAL ARTICLE**

SYNTHESIS OF RUTHENIUM COMPLEXES AND ASSESSING THEIR ANTICANCER AND ANTIBACTERIAL EFFECTS

ALI ZEIZ [1], SUZANNE CHAYYA [2], ZEINAB KASSEM [3], AKRAM HIJAZI [3], GHADA KHAWAJA [1], MOHAMMAD H. EL-DAKDOUKI [2]*

[1]*Department of Biological Sciences, Faculty of Science, Beirut Arab University, P.O. Box 11-5020, Riad El Solh 11072809, Beirut, Lebanon*
[2]*Department of Chemistry, Faculty of Science, Beirut Arab University, P.O. Box 11-5020, Riad El Solh 11072809, Beirut, Lebanon*
[3]*Doctoral School of Science and Technology, Platform for Research and Analysis in Environmental Sciences (PRASE), Lebanese University, Beirut, Lebanon*

**corresponding author: m.eldakdouki@bau.edu.lb*

Manuscript received: August 2023

Abstract

Ruthenium (Ru) complexes exhibit intriguing biological effects, including potent antibacterial and anticancer activities. The aim of this study was to prepare $Ru(dppz)(DMSO)_2Cl_2$ complex from *cis*-fac-dichlorotetrakis(dimethylsulfoxide)ruthenium(II) precursor (*cis*-$Ru(DMSO)_4Cl_2$), and assess its anticancer and antibacterial activities. The complex was characterized by NMR and FTIR spectroscopies. The physiochemical properties of the prepared complexes were predicted by employing MolSoft software and its DNA binding potential was assessed using molecular docking. The complex displayed an intercalative mode of DNA binding with a binding affinity of -15.93 kcal/mol and a hydrogen bonding of 2.5 Å. Additionally, Ru complex exhibited a promising antibacterial effect against *E. coli*, *E. faecalis*, *P. aeruginosa* and *S. aureus* at a minimum inhibitory concentration (MIC) of ~ 30 µg/mL. The cytotoxic activity of *cis*-$Ru(DMSO)_4Cl_2$ and $Ru(dppz)(DMSO)_2Cl_2$ complexes against colorectal (HCT-116) and breast cancer (MCF-7) cell lines was elucidated by using the MTT cell viability assay, and the latter complex displayed an intriguing low IC_{50} value (12.6 µM) in HCT-116 cells. The precise molecular mechanism of action of $Ru(dppz)(DMSO)_2Cl_2$ complex was deciphered by tracking the expression levels of key apoptotic proteins, namely p53, Bax and Bcl-2. Western blotting analysis showed that the anticancer activity is mediated by the complex's ability to activate the mitochondrial apoptotic pathway, as evident by modulating the expression level of p53, Bax and Bcl-2 proteins.

Rezumat

Complecșii ruteniului (Ru) prezintă efecte biologice variate, inclusiv activități antibacteriene și anticancerigene puternice. Scopul acestui studiu a fost dezvoltarea complexului $Ru(dppz)(DMSO)_2Cl_2$ din precursorul cis-fac-diclorotetrakis(dimetil-sulfoxid)ruteniu(II) (cis-$Ru(DMSO)_4Cl_2$) și evaluarea activităților sale anticanceroase și antibacteriene. Complexul a fost caracterizat prin metode spectroscopice de RMN și FTIR. Proprietățile fizico-chimice au fost determinate prin utilizarea *soft-ware*-ului MolSoft, iar potențialul de legare de ADN a fost evaluat folosind andocarea moleculară. Complexul s-a intercalat în structura ADN-ului cu o afinitate de legare de -15,93 kcal/mol și o legătură de hidrogen de 2,5 Å. În plus, complexul Ru a prezentat efect antibacterian împotriva *E. coli*, *E. faecalis*, *P. aeruginosa* și *S. aureus*, având o concentrație inhibitorie minimă (MIC) de ~ 30 µg/mL. Activitatea citotoxică a complexelor cis-$Ru(DMSO)_4Cl_2$ și $Ru(dppz)(DMSO)_2Cl_2$ asupra liniilor celulare colorectale (HCT-116) și de cancer de sân (MCF-7) a fost testată prin utilizarea testului MTT. De asemenea, a fost evaluată activitatea complexului asupra proteinelor p53, Bax și Bcl-2.

Keywords: $Ru(dppz)(DMSO)_2Cl_2$, molecular docking, Western blot, antibacterial effect

Introduction

Over the past decades, metal-based drugs have gained intense attention from the scientific community [1]. Metal-based cancer drugs have been introduced into clinical practice since the success of *cis*-$PtCl_2(NH_3)_2$, commonly known as cisplatin, in the treatment of various cancers, including ovarian, cervical, bladder, head and neck, melanoma and lymphoma [2]. Platinum-based chemotherapeutic drugs, mainly cisplatin and its derivatives carboplatin and oxaliplatin, exert their antitumour effect through inducing apoptosis and suppressing proliferation [3]. Additionally, substantial evidence suggested that the anticancer activity of platinum coordination complexes is attributed to their ability to cause DNA damage [4]. Such platinum-mediated DNA damage is well-documented to be associated with altered expression of various genes, thereby altering different intracellular signalling path-ways implicated in inflammation, differentiation and angiogenesis [5-7]. Despite their significant therapeutic value, the efficacy of cisplatin and its derivatives is limited, and are associated with a vast array of side effects, such as nausea and vomiting, myelosuppression,

immunosuppression, nephrotoxicity, neurotoxicity and hearing loss [3, 8]. Therefore, new metal-based anti-tumour drugs were investigated as potential alternatives to surmount the key limitations of platinum-based drugs [9].

Among the numerous metal-based compounds studied, ruthenium (Ru)-based drugs have attracted interest from researchers to treat tumours with selective cytotoxicity to cancer cells [10]. Similar to Pt(II), Ru(II) and Ru(III) ions have high affinity for nitrogen and sulphur donor ligands [11]. More importantly, ruthenium ions were shown to possess many advantages over platinum drugs, including higher efficacy, lower toxicity and lower drug resistance [12]. These effects have paved the way for the application of ruthenium derivatives in clinical studies [10, 12]. In particular, ruthenium complexes with heterocyclic N-donor ligands are the most prevalently studied drugs due to their photophysical and electrochemical properties [13], which rendered them applicable as photoactive DNA cleavage agents for therapeutic purposes [14].

Moreover, the study of transition metal complexes with sulfoxide ligands, mainly dimethyl sulfoxide (DMSO), expanded rapidly after the publication of the first article in 1960 [15]. A fundamental characteristic that makes these complexes worthy investigating is their use as precursors for the synthesis of a wide range of organometallic and coordination compounds [16]. From a chemical point of view, these compounds uniquely possess an isomerization bonding process due to the ambidentate behaviour of the sulfoxide ligand. Specifically, DMSO is a polar aprotic solvent thus making its complexes applicable for different studies without affecting their composition due to ligand exchange with the solvent [17]. It is worth noting that these complexes are useful in medical chemistry, and several metal complexes containing DMSO or other sulfoxide ligands exhibit antibacterial, antineoplastic and antimetastatic activities [18, 19]. For example, many studies have shown that $Ru(DMSO)_4Cl_2$ complexes exhibit remarkable antiproliferative and antimetastatic activities against various cancer cell lines [17, 20, 21].

Furthermore, transition metal complexes with dipyrido[3,2-a:2′,3′-c]phenazine (dppz) ligands have been extensively designed and assessed for their DNA-binding activity and therapeutic efficacy [22-24]. Dppz ligands are characterized by having a large aromatic surface area that allows efficient intercalation within the DNA base pairs [25]. As such, several Ru-dppz complexes were shown to exhibit significant antibacterial and anticancer effects [26, 27]. In this context, this study aimed at synthesizing and characterizing dichlorotetrakis (DMSO) ruthenium (II) $[RuCl_2(DMSO)_4]$ and dichlorobis (DMSO) (dipyrido-[3,2-a:2',3'-c]phenazine) $[RuCl_2(DMSO)_2(dppz)]$ complexes, and preliminarily assessing their antibacterial and anticancer effects.

Materials and Methods

Materials

Analytical grade DMSO, 1,10-phenanthroline, phenylene diamine, ruthenium(III) chloride hydrate ($RuCl_3.nH_2O$) and solvents were purchased from Sigma Aldrich and used as received without further purification. For antimicrobial assessments, *Staphylococcus aureus* (ATCC 25923), *Escherichia coli* (ATCC 10536), *Pseudomonas aeruginosa* (ATCC 10145), *Enterococcus faecalis* (ATCC 51299) were selected due to their clinical and pharmacological importance. Bacterial stock cultures were incubated for 24 hours at 37°C on nutrient agar and were subsequently stored at 4°C. Bacterial strains were grown in Mueller-Hinton agar (MHA) plates at 37°C. Bacteria was grown in nutrient broth at 37°C and maintained on nutrient agar slants at 4°C.

Regarding the anticancer activity assessment, human colorectal cancer cell line HCT-116 and human breast cancer cell line MCF-7(ER^+, $PR^{+/-}$, $HER2^-$) were used. These cell lines were cultured in Dulbecco's modified eagle's medium (DMEM) supplemented with 10% foetal bovine serum (FBS) and 100 U penicillin/streptomycin at 37°C and 5% CO_2 in a humidified chamber. All antibodies used in this study were purchased from Santa Cruz Biotechnology, California, Texas and involved anti-p53 (DO-1, mouse monoclonal IgG2a), anti-Bcl-2 (N-19, rabbit polyclonal IgG), anti-Bax (B-9, mouse monoclonal IgG2b) and secondary Horseradish Peroxidase (HRP)-conjugated antibodies. Both primary and secondary antibodies were diluted in 5% non-fat milk except for anti-β-actin antibody, which was diluted in TBS1X-0.001% Tween.

Synthesis of the ligands and complexes

*Synthesis of 1,10-phenanthroline-5,6-dione (**2**).* Compound **2** was synthesized according to the procedure reported by Yamada *et al*. [28]. In brief, 1,10-phenanthroline (1 g, 5.55 mmol) was mixed with KBr (1 g, 8.40 mmol) in an ice bath. A mixture of icy cold H_2SO_4/HNO_3 (10 mL/15 mL) was then added dropwise, and the reaction was subsequently refluxed for 3 hours. The hot yellow solution was then poured into 500 mL ice water and neutralized with NaOH where a yellowish milky solution formed. The desired product **2** was extracted by CH_2Cl_2 and the volatiles were evaporated under vacuum. The obtained solid was recrystallized from hot methanol, collected by suction filtration, and dried under vacuum to yield dione **2** in 77.6% yield (0.9 g).

*Synthesis of dppz ligand (**4**).* A mixture of **2** (0.5 g, 2.4 mmol) and 1,2-phenylene diamine **3** (0.398 g, 3.7 mmol) was dissolved in dimethylformamide (DMF). The reaction mixture was placed in an oil bath and refluxed for 4 hours, after which it was cooled to room temperature to produce a yellowish orange precipitate. The solid was collected by filtration,

washed with cold ethanol and vacuo dried. Dppz **4** was afforded in 74.6% yield (0.5 g).

Synthesis of $RuCl_2(DMSO)_4$ complex (5). Complex **5** was synthesized following the procedure described by Evans *et al*. [29], whereby ruthenium trichloride hydrate (0.5 g, 2 mmol) was refluxed in DMSO (3 mL) for 5 min until reducing the volume to half under vacuum. Acetone (10 mL) was then added to induce the formation of a yellow precipitate, which was subsequently filtered, washed with acetone and diethyl ether and dried under vacuum. The complex was recrystallized from hot DMSO to yield ruthenium complex **5** in 77% yield (0.75g).

*Synthesis of $Ru(dppz)Cl_2(DMSO)_2$ complex (**6**)*. $RuCl_2(DMSO)_4$ (0.1 g, 0.2 mmol) and dppz (0.056 g, 0.2 mmol) were dissolved in ethanol (30 mL). The mixture was maintained under reflux for 2 hours, and then cooled to room temperature to form a creamy white precipitate. The precipitate was filtered and dried under vacuum to yield the desired complex **6** in 57.5% (0.069 g).

Spectroscopic characterization

FTIR spectra of the prepared Ru complexes were obtained using a JASCO FT/IR-6300 spectrometer (400 - 4000 cm^{-1}). Solid-state spectra were recorded in KBr dispersed pellets. NMR spectra were recorded on a Bruker DSX-400 spectrometer. ^{1}H-NMR spectra were obtained on samples spun at the magic angle at ~ 10 kHz with a pulse time interval of 2 sec and pulse duration 2 μs. ^{13}C-NMR spectra were obtained on samples spun in the cross-polarization magic angle at ~ 5 kHz, with a pulse interval of 2 sec, a pulse duration of 3.5 μs and a contact duration between the H and the C of 5 ms. ^{13}C-DEPT-135 was also obtained to determine the presence of primary, secondary and tertiary carbon atoms in the prepared Ru complex.

Physiochemical characterization

Several physiochemical properties of the prepared complexes were determined by employing MolSoft (MolSoft, 2007) software, which represents physico-chemical parameters as numerical numbers. The assessed parameters were molecular weight (MW), the number of hydrogen bond acceptors (HBA), the number of hydrogen bond donors (HBD), partition coefficient (log P), solubility (log S), polar surface atoms (PSA), volume (VOL), percentage of absorption (%ABS), blood brain barrier (BBB) score and drug likeliness score (DLS).

Virtual screening via molecular docking

3D structures of Ru complexes were drawn and optimized by ChemSketch software, and subsequently docked with DNA segments Adenosine-Adenosine DNA Mismatch using AUTODOCK 4.2.6 software in order to screen for the basic DNA-ligand interactions. The prepared Ru complexes having conformational stability and structural diversity were docked with the crystal structure of 5 D (*CP*GP*GP*AP*AP*AP*TP*TP*AP*CP*CP*G)-3' DNA (PDB ID: 4E1U).

Antibacterial activity assessment

The prepared Ru complexes were screened for their *in vitro* antibacterial activity against four pathogenic bacterial strains, namely *E. coli*, *E. faecalis*, *P. aeruginosa* and *S. aureus*.

Determination of minimum inhibitory concentration

The minimum inhibitory concentration (MIC) of Ru complexes was determined using the broth dilution method. For that purpose, Ru complexes were dissolved in DMSO and serially diluted (two-fold) in broth medium until achieving a final concentration of DMSO less than 5%. Solutions containing Ru complexes were prepared at varying concentrations (5, 25, 50 and 100 μg/mL). Chloroxylenol was selected as a positive control and was dissolved in ultrapure water. All stock concentrations of complexes and antibiotic were filter-sterilized using 0.20 μm syringe filter. Two experimental protocols were followed. The first involved adding microbial suspensions (300 μL) and Ru complexes (300 μL) to each of the agars and incubated at 37°C for 24 hours. The second protocol involved adding the Ru complexes individually (300 μL) to agars during preparation, followed by the addition of microbial suspensions (300 μL) after cooling the agars to room temperature. Similar procedures were conducted for the positive control, while the negative control contained the test bacteria and sterile distilled water only. After incubation, the visual turbidity was detected and recorded. MIC was considered as the lowest concentration of Ru complexes at which the microbial colonies were completely absent.

Assessing bacterial susceptibility to Ru complexes

The susceptibility of the tested bacterial strains to the Ru complexes was evaluated by the disk diffusion assay and measuring the zones of growth inhibition. Amoxicillin, chloramphenicol, streptomycin and tetracycline were selected as positive controls for anti-bacterial assessment. Ru complexes at a concentration of 30 μg/mL (based on MIC) and standard antibiotic drugs were diluted in double-distilled water using nutrient agar tubes. Mueller-Hinton sterile agar plates were seeded with indicator bacterial strains (10^8 CFU) and allowed to incubate at 37°C for 3 hours. The zones of growth inhibition around the disks were measured after 18 - 24 hours of incubation at 37°C for bacteria. The sensitivity of bacterial strains to the prepared Ru complexes was determined by measuring the sizes of inhibitory zones (including the diameter of disk) on the agar surface around the disks, and values < 8 mm were considered as not active against bacteria.

Anticancer activity assessment

Antiproliferative activity. The MTT (3-(4,5-dimethyl-thiazol-2-yl)-2,5-diphenyltetrazolium bromide) cell viability assay was used to assess the antiproliferative activity of the complexes. Briefly, HCT-116 and MCF-7 (ER^+, $PR^{+/-}$, $HER2^-$) cells were seeded in 96-well

plates at a concentration of 2 x 10^5 cells/mL and allowed to grow. Cells were treated with varying concentrations of drug complexes for 48 hours against a negative control. Following the treatment period, cell viability was measured by adding 10 µL of MTT reagent to the plates, which were then incubated in a humidified incubator at 37°C (95% air, 5% CO_2) for two hours. Quantitation of the formed formazan crystals was calorimetrically recorded at 570 nm against a blank. The percentage of cell viability was reported correspondingly by dividing the average absorbance of the complex treated cells by the control of non-treated cells. Viability graphs were plotted as % viable cells *versus* drug concentration (logarithmic scale) for determining the IC_{50} (drug concentration at which 50% of the cells are viable relative to the control).

Western blotting. Protein expression levels were assessed following the migration of equal protein concentrations in a 12% sodium dodecyl sulphate (SDS)-polyacrylamide gel electrophoresis in three independent Western blot assays. Cell extracts were prepared by adequate dilution in distilled water and a constant 10 µL volume of Laemmli loading buffer (0.25 M Tris-HCl, pH 6.8; 4% SDS; 20% glycerol; bromophenol blue and 5% β-mercaptoethanol). The lysates were loaded into the gel and allowed to stack for 30 minutes at 50 V, followed by migration in the resolving gel at 100 V. Proteins were then transferred into a 0.45 mm nitrocellulose membrane in methanol transfer buffer for 2 hours at a constant voltage of 50 V. Following overnight blocking in 5% non-fat milk at 4°C, membranes were incubated with primary antibodies anti-p53, anti-Bcl-2 and anti-Bax for 2 hours at room temperature. For loading controls, anti-β-actin antibody was used. Membranes were then washed 6 times for 5 minutes in TBS1X-0.001% or 0.0002% Tween at room temperature, followed by 1-hour incubation with adequate secondary horseradish peroxidase (HRP)-conjugated antibodies. Both primary and secondary antibodies were diluted in 5% non-fat milk, except for anti-β-actin antibody, which was diluted in TBS1X-0.001% Tween. Protein expression signals were then visualized on the developed membrane using Clarity Western enhanced chemiluminescence (ECL) blotting substrate (Bio-Rad) on the ChemiDoc imaging system (Bio-Rad).

Statistical analysis

All data are represented as mean ± standard deviation. Data was analysed by one-way ANOVA test for multiple comparisons and unpaired Student's *t* test using Graph Pad Prism 6 software. Values considered statistically significant for p-value ≤ 0.05.

Results and Discussion

Synthesis and characterization of Ru(II) complexes

The synthetic route (Figure 1) leading to the preparation of the Ru(II) complexes started by the preparation of the dppz ligand **4** *via* oxidation of 1,10-phenanthroline (**1**) in HNO_3/H_2SO_4 under reflux conditions to yield 5,6-dione **2** [28], which was further reacted with *o*-phenylene diamine to afford the desired ligand. The synthesis of Ru(dppz)$(DMSO)_2Cl_2$ complex **6** was achieved by reacting *cis*-Ru$(DMSO)_4Cl_2$ complex and dppz ligand. *cis*-Ru$(DMSO)_4Cl_2$ complex **5** constituted a suitable ruthenium source because of its empirically proven anticancer activity and stable octahedral geometry [30], in addition to the ease of displacing two DMSO ligands with a single bidentate ligand such as dppz [31]. In fact, the large aromatic surface area on the dppz ligand permitted the feasible coordination to the metal centre [27]. Therefore, *cis*-Ru$(DMSO)_4Cl_2$ **5** was accessed by refluxing $RuCl_3$ hydrate in DMSO following a well-established method [29]. Simple ethanolic reflux of **5** with dppz ligand **4** yielded the desired Ru(dppz)$(DMSO)_2Cl_2$ **6** in acceptable yield (Figure 1). Spectroscopic analysis by NMR and FTIR confirmed the successful synthesis of the ruthenium complexes.

Particularly, the ^{1}H-NMR spectrum of Ru(dppz)$(DMSO)_2Cl_2$ showed the presence of characteristic peaks of the dppz ligand as evident by the downfield peaks between 7.00 to 9.37 ppm (Figure 2a). These peaks correspond to the aromatic protons of the ligand, thereby proving its presence in the complex. The ^{13}C-NMR spectrum of Ru(dppz)$(DMSO)_2Cl_2$, showed the presence of 18 peaks in the region 127 - 155 ppm, suggesting the presence of one dppz ligand connected to Ru(II) core. Eight of these peaks corresponded to the quaternary carbon atoms as they disappeared in the ^{13}C-DEPT-135 spectrum, while the other 10 peaks corresponded to the aromatic C-H (Figure 2b). Asymmetry in the ^{13}C-NMR is probably due to the chelation of two DMSO molecules, which expresses different magnetic effect on the dppz ligand chelated to the ruthenium compound. Thus, the primary structural characterization by NMR analysis were in agreement with the composition anticipated for the complexes.

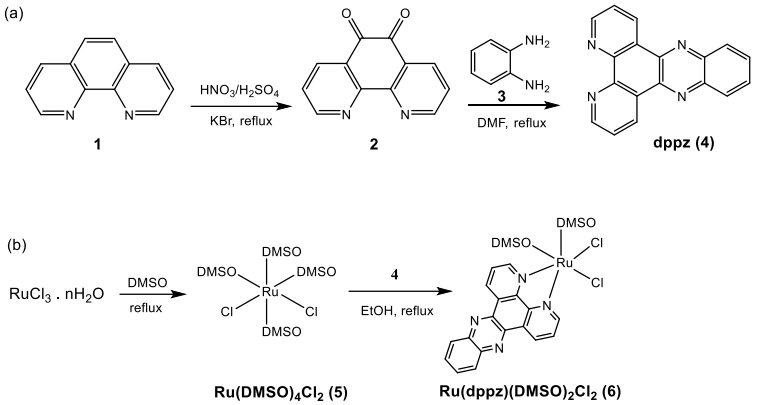

Figure 1.

Preparation of the complexes: (a) dppz ligand, (b) $Ru(DMSO)_4Cl_2$ and $Ru(dppz)(DMSO)_2Cl_2$

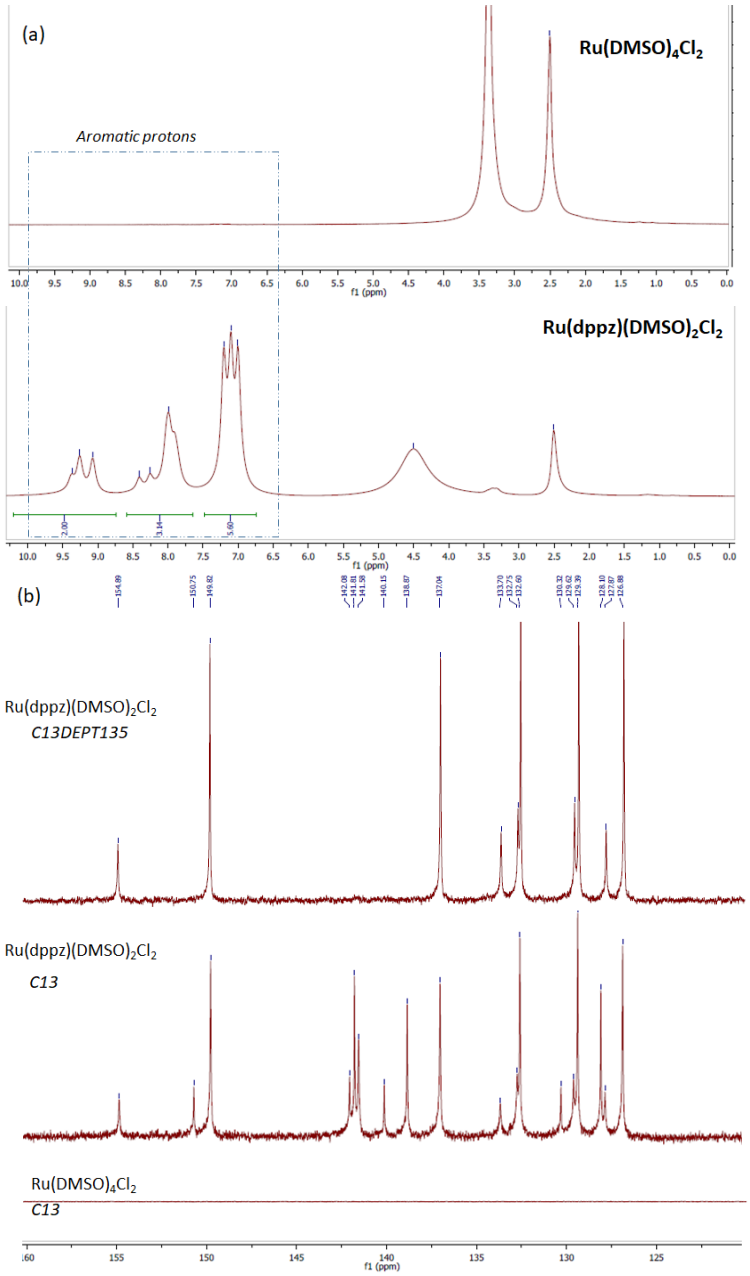

Figure 2.

The $Ru(DMSO)_4Cl_2$ and $Ru(dppz)(DMSO)_2Cl_2$ complexes recorded spectra: (a) ^{1}H-NMR and (b) ^{13}C-NMR

FTIR spectroscopy provided a better understanding of the coordination of DMSO and dppz to the Ru centre and validate their binding mode. As shown in Figure 3, $Ru(DMSO)_4Cl_2$ complex exhibits a characteristic peak at 1080 cm^{-1} that corresponds to the Ru–S-bonded DMSO [30] and suggested the coordination of DMSO molecules within the Ru centre. The presence of bands between 3000 cm^{-1} and 3200 cm^{-1} characteristics of =C–H stretching vibrations supported the successful coordination of dppz to Ru centre. These bands are absent in the spectrum of *cis*-$Ru(DMSO)_4Cl_2$. On the other hand, the presence of DMSO ligands in both complexes is evidenced by the bands between 2850 cm^{-1} and 2950 cm^{-1} attributed to the C–H stretching vibrations in the methyl groups of DMSO, as well as by the two strong bands at ~ 1106 cm^{-1} and 1014 cm^{-1} assigned to the stretching of the S=O bond. The latter absorption bands signalled that DMSO is *S*-bonded to the metal core rather than *O*-bonded since *O*-bonded DMSO would be expected to appear at around 930 cm^{-1} [32]. These bands became less intense in the IR spectrum of $Ru(dppz)(DMSO)_2Cl_2$ indicating the replacement of some DMSO molecules by dppz ligand.

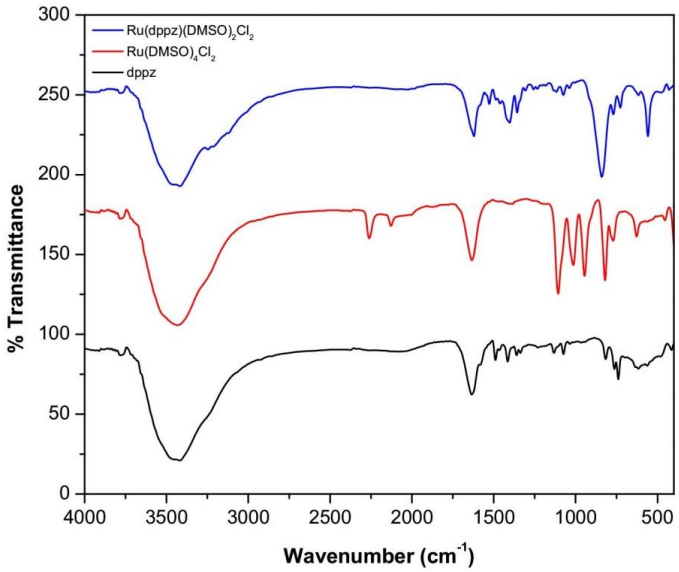

Figure 3.
FTIR spectrum of dppz, $Ru(DMSO)_4Cl_2$ and $Ru(dppz)(DMSO)_2Cl_2$ complexes

Physiochemical characteristics

The development of metal-based complexes as medicinal agents is chiefly influenced by multiple physicochemical properties. For instance, a reduced molecular flexibility (as assessed by the number of rotatable bonds), a low polar surface area and a high total hydrogen bond count (the sum of donors and acceptors) are all critical predictors of improved oral bioavailability [1]. Additionally, membrane permeability and bioavailability are usually linked to fundamental molecular characteristics, such as partition coefficient (logP), molecular weight (MW) and the number of hydrogen bond acceptors (HBA) and donors (HBD) in a molecule [33]. In the present study, the physiochemical parameters of $Ru(DMSO)_4Cl_2$ (**5**) and $Ru(dppz)(DMSO)_2Cl_2$ (**6**) were elucidated using a molecular modelling software (MolSoft) and the results are enlisted in Table I.

Table I
Physiochemical properties of the prepared Ru complexes predicted using MolSoft (2007) software

Physiochemical properties	**cis-$Ru(DMSO)_4Cl_2$**	**$Ru(dppz)(DMSO)_2Cl_2$**
Molecular Formula	$C_8H_{30}Cl_2O_4RuS_4$	$C_{22}H_{48}Cl_2N_4O_2RuS_2$
MW	489.94	636.13
HBA	4	4
HBD	6	8
LogP	-6.99	-3.48
LogS	0.2	0.17
PSA	82.21	76.04
VOL	223.05	452.8
%ABS	80.638	82.766
BBB	2.19	2.38
DLS	-1.29	-1.26

In general, a logP coefficient less than 5, a molecular weight less than 500, a number of HBAs less than 10 and a number of HBDs less than 5 are all characteristics of molecules with potentially high membrane permeability. These characteristics are known as "rule-of-five" or "Lipinski's rule of drug-likeness" [34]. The hydrogen-bonding capability is recognized as a key factor in determining medication permeability. Commonly, when a compound has more than 5 HBDs and 10 HBAs, it is more likely to have a poor oral bioavailability. Results of the present study showed that the prepared Ru(II) complexes **5** and **6** have logP values less than 5 (-6.99 and -3.48, respectively). They were also shown to possess 4 HBAs (< 5), but 6 and 8 HBDs (< 10), respectively. Furthermore, compound solubility (assessed as logS) is a critical parameter that determines compound's transition from the administration state to the level of reaching the bloodstream. Insufficient solubility of medications is widely recognized as an underlying cause of inadequate absorption [33]. Our findings showed relatively high logS of 0.2 mol/L for $Ru(DMSO)_4Cl_2$ and 0.17 mol/L for $Ru(dppz)(DMSO)_2Cl_2$. Collectively, these values indicated that both complexes meet the criteria of good absorption of compounds.

The polar surface area (PSA) is the sum of the surfaces of polar atoms in a molecule (typically oxygen, nitrogen and connected hydrogen). It is a highly valuable parameter for predicting compound transport characteristics [35]. Ideally, molecules with PSA less than 120 Å have good oral bioavailability. The prediction model applied in the current study calculated PSA of 82.21 Å for $Ru(DMSO)_4Cl_2$ and 76.04 Å score for $Ru(dppz)(DMSO)_2Cl_2$. These values are considered suitable for compounds with high oral bioavailability. Absorption, measured as percent absorption (%ABS), is used to represent the magnitude of the molecule's translocation from the intestines to the blood circulation. The %ABS ranged from 80.63% for $Ru(DMSO)_4Cl_2$ to 82.76% for $Ru(dppz)(DMSO)_2Cl_2$, thereby indicating that both complexes are highly absorbed and translocated. It is worth noting that PSA and volume (VOL) are inversely related to %ABS [33], where molecules with high PSA being polar, and therefore, have lower tendency the cross the cell membranes of the cells making up the intestine lining.

The ideal drug-likeness score (DLS) for a potential drug is 1, and any substance with a DLS close to unity is deemed to have drug-like properties [36]. The calculated DLS score for $Ru(DMSO)_4Cl_2$ and $Ru(dppz)(DMSO)_2Cl_2$ complexes are -1.29 and -1.26, respectively. Another important parameter that provides valuable insights into the ability of a given medication to cross the blood brain barrier (BBB) and reaches the brain cells is the BBB score. Given that a BBB score between 0 and 6 is said to be optimal [37], $Ru(DMSO)_4Cl_2$ and $Ru(dppz)(DMSO)_2Cl_2$ complexes had scores of 2.19 and 2.38, indicating their ability to cross the BBB. The overall evaluation of the physiochemical characteristics for Ru(II) complexes suggested that they are readily absorbed upon oral administration and can be considered candidate lead molecules with acceptable drug-like characteristics.

Virtual screening via molecular docking

Molecular docking is an appealing technique that sheds light into drug-biomolecule interactions. Specifically, DNA is considered a potential target for metal-based drugs [38]. To gain insights into the DNA binding mode of the prepared Ru complexes and their most probable binding site, molecular docking studies were performed under the assumption that DNA and Ru complexes are rigid. The molecular docking technique is of utmost importance as it can contribute to rational drug design and mechanistic studies by placing a small molecule into the binding site of the DNA target region, mainly in a non-covalent mode [39]. In this work, docking studies have been performed on the prepared complexes with B-DNA (PDB ID: 4E1U) 5'-D (*CP*GP*GP*AP*AP*AP*TP*TP*AP*CP*CP*G)-3' to explore the most feasible binding site, interaction mode and binding affinity.

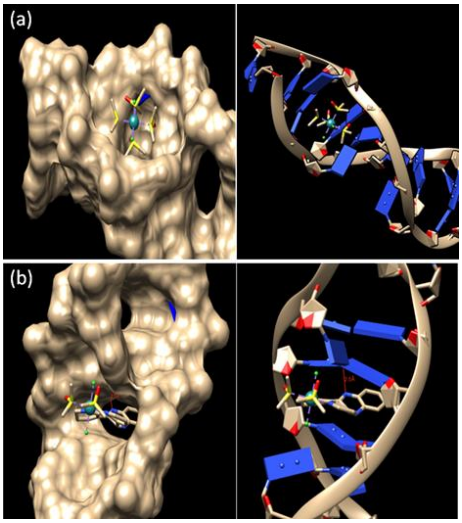

Figure 4.
Binding pose of the complexes in the binding site in DNA 4E1U: (a) $Ru(DMSO)_4Cl_2$ and (b) $Ru(dppz)(DMSO)_4Cl_2$;
(hydrogen bond in (b) is shown in red colour)

As shown in Figure 4, $Ru(DMSO)_4Cl_2$ and $Ru(dppz)(DMSO)_2Cl_2$ complexes interacted with DNA through partial intercalation at the major groove. The resulting relative binding energies of docked complexes with DNA are -8.81 and -15.93 kcal/mol for $Ru(DMSO)_4Cl_2$ and $Ru(dppz)(DMSO)_2Cl_2$ complexes, respectively. In fact, higher negative binding energy suggests stronger DNA-binding affinity [39]. Thus, it can be deduced that the DNA-binding affinity of $Ru(dppz)(DMSO)_2Cl_2$ complex is better than that of $Ru(DMSO)_4Cl_2$. The higher binding affinity of complex $Ru(dppz)(DMSO)_2Cl_2$ can be rationalized by the

presence of a stabilizing hydrogen-bonding interaction between the complex and DNA with a length of 2.5 Å. Our findings regarding the molecular docking of $Ru(DMSO)_4Cl_2$ complex are in agreement with previous molecular docking studies that were employed to understand the DNA-binding mode of this complex [40]. Similarly, previous molecular docking reports have shown an intercalative mode of binding between various Ru complexes and DNA base pairs, such as Ru(II)-polypyridyl complexes [41, 42], Ru(II)-hydrazone complexes [43] and Ru(II)-chalcone complexes [44]. More importantly, our findings are consistent with similar studies involving Ru complexes with dppz ligands, such as $[Ru(bpy)_2dppz\text{-}idzo]^{2+}$ [45] and $[Ru(bpy)_2dppz]^{2+}$ [46], which are well-documented for their ability to bind to DNA's major groove and to be stabilized by hydrogen bonding [27].

Assessing antibacterial activity

Antibacterial studies were performed on two Gram-positive (*E. faecalis* and *S. aureus*) and two Gram-negative (*E. coli* and *P. aeruginosa*) bacteria. The MIC of the prepared Ru complexes was determined using the microdilution agar method, where four concentrations (5, 25, 50 and 100 μg/mL) of each complex were tested. The antibacterial activity of the Ru(II) complexes was compared to 1% chloroxylenol, a commercial antibiotic used as a positive control in the current study, and results are summarized in Table II. Remarkably, the dppz-based complex **6** showed a better antibacterial activity against all tested bacterial strains with a lower MIC of 50 μg/mL compared to 100 μg/mL for complex **5**.

Table II

Number of colonies of bacterial strains treated with Ru complexes at different concentrations. MIC was determined as the lowest complex concentration that did not result in visual growth of microorganisms

Test compound	Concentration	Number of Colonies			
		E. coli	***E. faecalis***	***P. aeruginosa***	***S. aureus***
Negative control	0	147.5 ± 3.64	150 ± 3.81	140.5 ± 2.96	167.25 ± 3.03
Chloroxylenol	1%	0	0	0	0
$Ru(DMSO)_4Cl_2$ (μg/mL)	5	45.75 ± 3.03	60.25 ± 2.59	64.5 ± 3.35	69.25 ± 3.03
	25	16.25 ± 3.34	30.25 ± 2.59	30.00 ± 2.92	39.25 ± 2.86
	50	3.75 ± 2.38	2.75 ± 1.30	5.00 ± 2.24	6 ± 2.24
	100	0	0	0	0
$Ru(dppz)(DMSO)_2Cl_2$ (μg/mL)	5	18.25 ± 2.59	35.25 ± 3.49	50.00 ± 3.39	35.5 ± 4.15
	25	9.00 ± 1.87	11.00 ± 1.87	7.25 ± 1.48	4.75 ± 1.92
	50	0	0	0	0
	100	0	0	0	0

Measurements were done in triplicates

In addition, the MIC for the Ru(II) complexes was determined from a different experimental set-up to assess their utility in preventing bacterial infections. In specific, the Ru complexes were added at different concentrations into the preparation of growth media before culturing the bacterial strains on the agar plates. The obtained results, presented in Table III, corroborated those observed in the first setup where MIC of 50 μg/mL and 100 μg/mL were obtained for the Ru (II) complexes, respectively, against all bacterial strains. It is worth remarking that our reported antibacterial activity is comparable to what was described for other dppz-based Ru complexes, such as the $[RuCl(CO)(dppb)(dppz)]PF_6$ complex (20 μg/mL) [47] and the $[Ru(2,9\text{-}Me_2phen)_2(dppz)]^{2+}$ complex (26 μg/mL) [48]. Further, our results are better than those obtained by Liu *et al*. [49], who reported noticeable activity for $[Ru(phen)_2(dppz)]^{2+}$ complex (64 - 128 μg/mL) against Gram-negative bacteria.

Table III

Number of colonies of bacterial strains pre-treated with Ru complexes at different concentrations. MIC was determined as the lowest complex concentration that did not result in visual growth of microorganisms

Test compound	Concentration	Number of Colonies			
		E. coli	***E. faecalis***	***P. aeruginosa***	***S. aureus***
Negative control	0	129.50 ± 3.64	149.50 ± 2.95	140.75 ± 2.68	169.25 ± 3.34
Chloroxylenol	1%	0	0	0	0
$Ru(DMSO)_4Cl_2$ (μg/mL)	5	45.00 ± 4.12	55.25 ± 3.49	44.00 ± 3.39	31.50 ± 4.92
	25	10.00 ± 2.73	4.75 ± 1.92	4.00 ± 2.24	7.75 ± 1.92
	50	0	0	0	0
	100	0	0	0	0
$Ru(dppz)(DMSO)_2Cl_2$ (μg/mL)	5	24.75 ± 3.96	34.50 ± 2.95	26.50 ± 4.39	39.50 ± 2.96
	25	2.00 ± 1.22	2.50 ± 1.11	3.00 ± 1.58	3.25 ± 1.92
	50	0	0	0	0
	100	0	0	0	0

Measurements were done in triplicates

The antibacterial activity of the prepared Ru complexes was further assessed using the disc diffusion assay at a concentration of 20 μM and compared to that of reference antibiotics (Table IV and Figure 5). $Ru(DMSO)_4Cl_2$ complex induced zones of growth inhibition between 10.2 mm and 15.7 mm which are comparable to those obtained using amoxicillin (9.6 - 20.1 mm). At the same tested concentration, $Ru(dppz)(DMSO)_2Cl_2$ complex exhibited a stronger antibacterial activity and induced zones of growth inhibition in the range 16.7 - 19.7 mm. The antibacterial activity of $Ru(dppz)(DMSO)_2Cl_2$ complex was comparable to several commercial antibiotics such as amoxicillin, streptomycin and tetracycline (Table IV).

Table IV

Zones of bacterial growth inhibition by Ru complexes and some clinically used antibacterial agents against some bacterial strains

Test Compound	Concentration/μg	Diameter of growth inhibition zone (mm)			
		E. coli	*E. faecalis*	*S. aureus*	*P. aeruginosa*
Amoxicillin	30	17.5 ± 0.607	20.1 ± 0.426	9.60 ± 0.506	14.5 ± 0.491
Streptomycin	10	16.1 ± 0.210	21.6 ± 0.611	19.5 ± 0.790	15.9 ± 0.486
Tetracycline	30	15.2 ± 0.421	19.0 ± 0.253	18.6 ± 0.491	19.8 ± 0.306
Chloramphenicol	30	20.9 ± 0.253	20.9 ± 0.827	21.7 ± 0.850	18.5 ± 0.548
$Ru(DMSO)_4Cl_2$	20	11.8 ± 0.943	15.7 ± 0.486	10.2 ± 0.219	13.8 ± 0.253
$Ru(dppz)(DMSO)_2Cl_2$	20	17.8 ± 0.643	19.7 ± 0.556	16.7 ± 0.599	17.7 ± 0.491

Experiments were done in triplicates, and values were reported as mean ± standard deviation

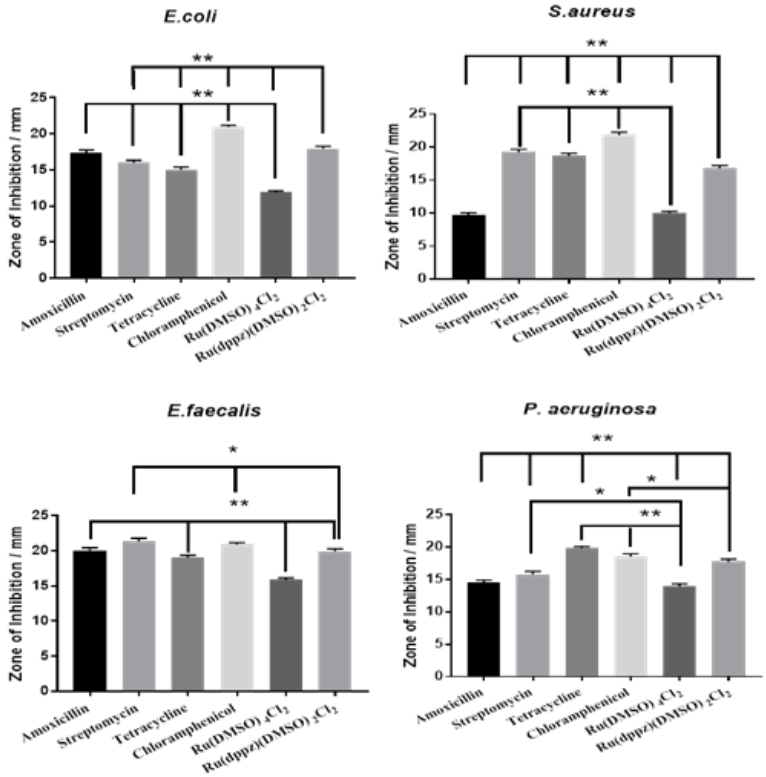

Figure 5.

Statistical analysis of the zones of bacterial growth inhibition. Data are represented as mean ± SEM, statistical significance was assessed using Student's t-test (* $p < 0.05$; ** $p < 0.01$; *** $p < 0.001$) for activity between $Ru(DMSO)_4Cl_2$ and $Ru(dppz)(DMSO)_2Cl_2$

The promising activity of our novel $Ru(dppz)(DMSO)_2Cl_2$ complex could be attributed to the fact that Ru complexes are usually positively charged, which allows their interaction with several bacterial targets, such as phospholipids located in the bacterial membrane and cell wall [50]. Moreover, it is important to note that chelation increases the ability of complexes to permeate microorganisms' cell membranes through reducing the polarizability of the metal [51]. The $Ru(dppz)(DMSO)_2Cl_2$ complex is apparently more lipophilic than its precursor $Ru(DMSO)_4Cl_2$ complex due to the phenyl rings in the dppz ligand. Therefore, penetration through bacterial cell wall is much more

conceivable than with the $Ru(DMSO)_4Cl_2$ complex, leading to greater zones of bacterial growth inhibition. Nevertheless, measuring Ru uptake is warranted to confirm such justification. Furthermore, $Ru(dppz)(DMSO)_2Cl_2$ is more effective against Gram positive and negative bacteria than $Ru(DMSO)_4Cl_2$, despite both compounds having an antibacterial action. In fact, ruthenium(II) complexes have been shown to bind DNA and RNA in live bacteria. As bacterial DNA and RNA are located in the cytoplasm of the microorganisms rather than the nucleus [52], they are more susceptible to intercalation by the ruthenium complexes [49], which is what gives these compounds their antibacterial effect.

The capacity of $Ru(dppz)(DMSO)_2Cl_2$ to bind to nucleic acids through intercalation will also increase in the presence of dppz compared to $Ru(DMSO)_4Cl_2$ precursor probably through π-π stacking with the nucleic acid bases. As a result, dppz play a critical role in increasing the activity of $Ru(dppz)(DMSO)_2Cl_2$ by increasing the ability of interaction and binding to DNA and RNA, resulting in enhanced bactericidal activity [49].

Cytotoxic activity

The cytotoxicity profiles of the prepared Ru complexes were assessed using human carcinoma cell lines, namely HCT-116 (colorectal) and MCF-7 (breast). Colorectal and breast cancers are among the most intimidating causes of death worldwide [53]. Although platinum (Pt)-based anticancer drugs have been commonly used to treat these cancers, their toxicity and development of resistance by cancer cells have piqued interest in using Ru-based drugs as alternatives [54]. In general, most of the studied Ru complexes are cytotoxic against these types of cancers, with IC_{50} values ranging from 10 μM to 50 μM [55]. The resulting dose-response curves obtained following treatment for 48 h are depicted in Figure 6, and the corresponding cytotoxic potency (expressed as IC_{50} values) is summarized in Table V. The cytotoxicity of the tested complexes was found to be concentration dependent. In general, $Ru(DMSO)_4Cl_2$ showed moderate cytotoxicity against both human cancer cell lines with IC_{50} values of 45.8 μM and 54.6 μM in HCT-116 and MCF-7 cell lines, respectively. In contrast, $Ru(dppz)(DMSO)_2Cl_2$ demonstrated stronger cytotoxic activity than $Ru(DMSO)_4Cl_2$ against both cell lines, whereby it exhibited IC_{50} values of ~ 12.6 and 13.6 in HCT-116 and MCF-7 cell lines, respectively (Table V). Our findings agree very well with previous studies showing that Ru(II) complexes containing dppz exert an enhanced anticancer activity against cancer cells [26, 27]. The high cytotoxicity of $Ru(dppz)(DMSO)_2Cl_2$ could be attributed to the lipophilicity of the dppz ligand, given that the cytotoxicity of several metal-based anticancer complexes increases with an increase in their lipophilicity [56]. Furthermore, several studies reported that lipophilicity (log P value) of Ru-based complexes is positively correlated to higher cellular uptake, which results in higher cytotoxicity [57, 58].

Table V

IC_{50} (μM) values for $Ru(DMSO)_4Cl_2$ and $Ru(dppz)(DMSO)_2Cl_2$ complexes in HCT-116 and MCF-7 cell lines. Statistical significance was assessed by Student's two-tailed t test.

Complexes	IC_{50} (μM)	
	HCT-116	MCF-7
$Ru(DMSO)_4Cl_2$	45.80 ± 0.48^a	54.60 ± 0.35^a
$Ru(dppz)(DMSO)_2Cl_2$	12.60 ± 0.40^b	13.57 ± 0.43^b

Different superscript letters in the same column indicate significant difference ($p < 0.01$)

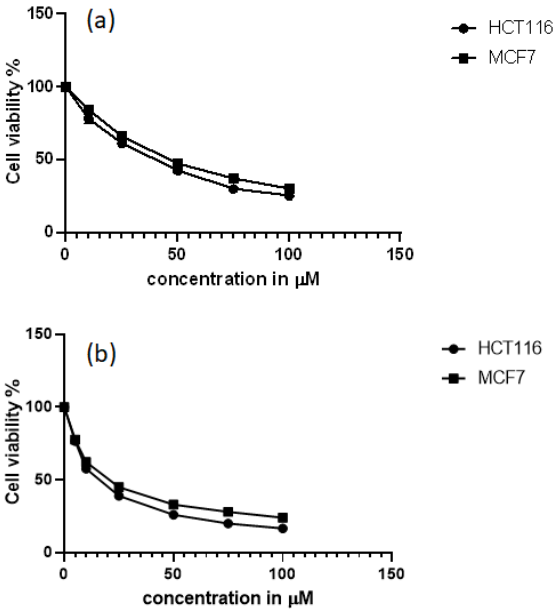

Figure 6.

Dose-response curve of the complexes at different concentrations in HCT-116 and MCF-7 cell lines: (a) $Ru(DMSO)_4Cl_2$ and (b) $Ru(dppz)(DMSO)_2Cl_2$
OD was measured after 48 hours of treatment and compared to untreated cells (control)
Experiments were done in triplicates and data is reported as mean ± standard deviation

Ruthenium compounds are known to bind to DNA with a high degree of selectivity. By hydrolysing their ligands, the electron-deficient metal atoms in these complexes could serve as electron acceptors for electron-rich DNA nucleophiles. In addition, metal-based drugs with ligands characterized by wide planar aromatic surfaces (such as dppz) can intercalate between the base pairs of double-stranded DNA and form stable complexes through non covalent interactions such as π-π stacking, Van der Waals forces, hydrophobic interactions and electrostatic attractions [59]. In fact, the strong binding affinity of the intercalator with DNA stabilizes the latter's double helix structure and effectively disrupt the binding of the nuclear factor-κB (NF-κB) transcription factor to DNA sequences, limiting cellular transcription and causing irreversible cancer cell death [60, 61]. Studies by linear and circular

dichroism spectroscopies revealed that upon intercalation of dppz ligand between the base pairs, the Ru complex binds from the minor groove thus corroborating the results of the molecular docking experiments conducted in the current study [62].

Western blotting analysis

Although the prepared dppz-containing Ru complex exhibited higher cytotoxicity against HCT-116 and MCF-7 cell lines, the precise molecular mechanisms of action of this complex are warrant exploring to decipher the mode of cell death. In general, cell death can be caused by apoptosis, necrosis, or autophagy. Apoptosis is mainly induced by the activation of the internal or external (death receptor mediated) pathways. The internal pathway, also called the mitochondria mediated pathway, is triggered by DNA damage, oxidative stress and endoplasmic reticulum (ER) stress. These stimuli induce the release of cytochrome C from the mitochondria leading to the activation of various apoptotic proteins. A growing body of evidence suggests that Ru(II) complexes potentially induce cancer cell death *via* apoptosis [63-65]. Thus, aiming to assess the apoptotic potential of our novel $Ru(dppz)(DMSO)_2Cl_2$ complex against HCT-116 cells, its effect on the expression levels of some key proteins in the internal apoptotic pathway, namely p53, Bax and Bcl-2, was investigated using Western blotting.

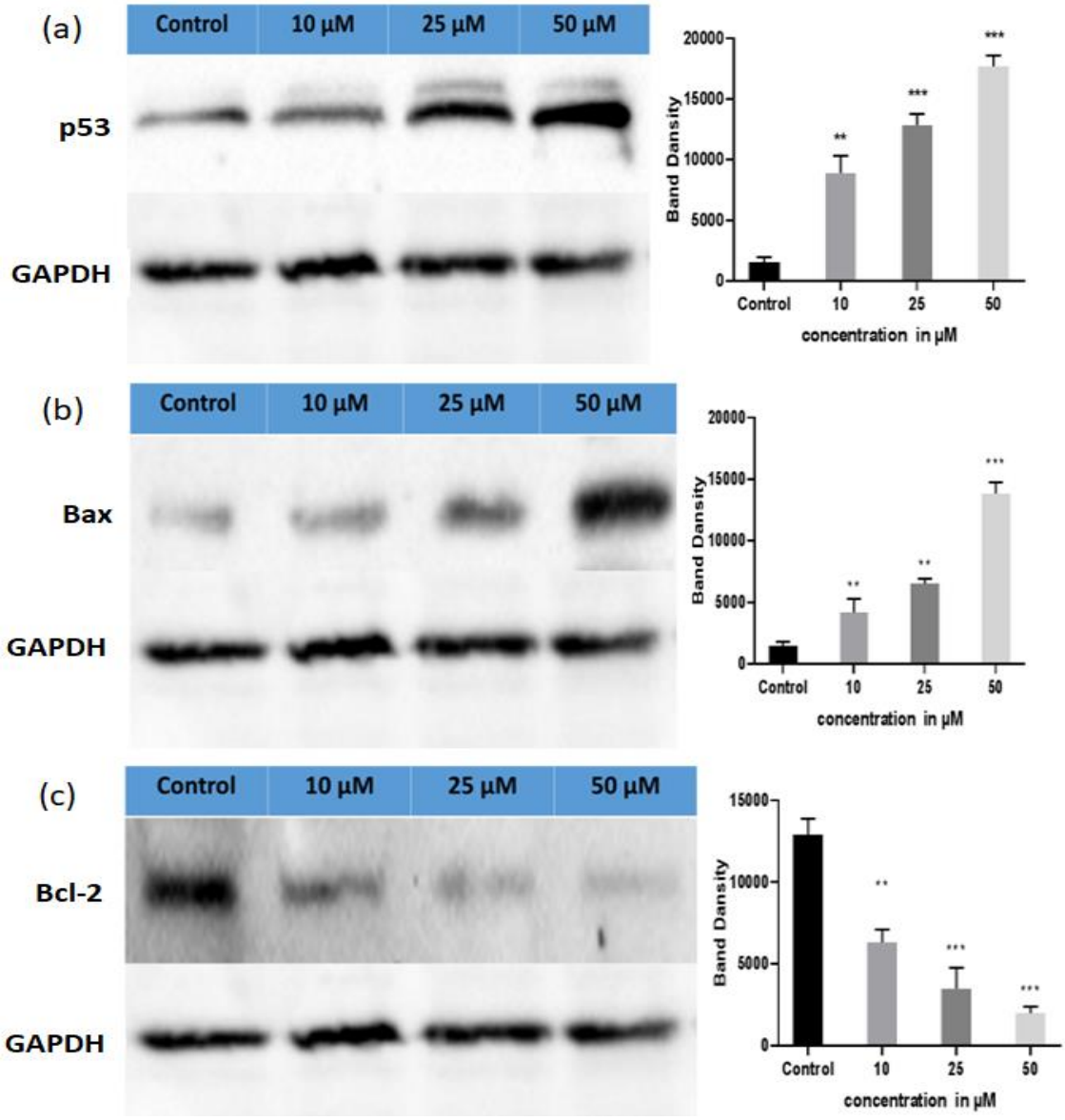

Figure 7.

Western blot analysis of the protein expression levels in control and $Ru(dppz)(DMSO)_2Cl_2$-treated HCT-116 cells:(a) p53, (b) Bax and (c) Bcl-2

Results are presented as average fold-change in protein level normalized to GAPDH. Data are presented as mean ± standard deviation. Statistical significance was assessed using Student's t-test (* $p < 0.05$; ** $p < 0.01$; *** $p < 0.001$) for band density between different concentration of $Ru(dppz)(DMSO)_2Cl_2$ and control

The tumour suppressor protein p53 plays a fundamental role in cellular response to DNA damage [66]. p53 plays a prominent role as a facilitator of DNA repair by halting the cell cycle to allow time for the repair machineries to restore genome stability [67]. Therefore, targeting p53 activity is regarded as an important strategy in cancer therapy as its overexpression is implicated in the inhibition of cancer cells' division and growth [68]. As shown in Figure 7a, treating HCT-116 cells to 5 - 50 μM of complex $Ru(dppz)(DMSO)_2Cl_2$ for 24 h resulted in a noticeable dose-dependent increase in p53 levels. This implies that cell apoptosis or DNA damage was triggered in HCT-116 cells upon treatment with the dppz-based ruthenium complex.

In order to confirm that $Ru(dppz)(DMSO)_2Cl_2$ - induced activation of p53 is associated with activating the mitochondrial pathway in apoptosis, Western blotting analysis was performed for Bax and Bcl-2. Previous studies have demonstrated that p53 promotes the transcription of the pro-apoptotic protein Bax, which regulates the release of cytochrome C from the mitochondria and results in cell apoptosis by activating caspase-3 and caspase-9 [69]. In contrast, Bcl-2 is an anti-apoptotic protein that governs mitochondrial outer membrane permeabilization and suppresses apoptosis [70]. Similar to p53 results, Bax level was found to be dose-dependently upregulated in HCT-116 cells treated with $Ru(dppz)(DMSO)_2Cl_2$ as shown in Figure 7b. On the other hand, Bcl-2 was dose-dependently down-regulated in HCT-116 cells following treatment by the same complex (Figure 7c). These results suggested that $Ru(dppz)(DMSO)_2Cl_2$ upregulates p53 level and its downstream target gene Bax while it downregulated that of Bcl-2. Such changes impair mitochondrial outer membrane permeabilization leading to the release of cytochrome C, an apoptosis-inducing factor, into the cytosol, which induces apoptotic cell death of cancer cells. Collectively, these findings demonstrated that the mitochondrial pathway was implicated in cellular apoptosis driven by $Ru(dppz)(DMSO)_2Cl_2$ complex.

Conclusions

The majority of the physiochemical characteristics of the Ru complex were desirable, suggesting relatively high drug likeness that supports our results. Interestingly, the complex exhibited an intercalative mode of DNA binding, rendering DNA a potential biological target for this complex. Biological investigations showed a remarkable antibacterial activity of this complex against Gram-positive (*E. faecalis* and *S. aureus*) and Gram-negative (*E. coli* and *P. aeruginosa*) bacterial strains. Moreover, the anticancer activity of this complex was perceived against colorectal and breast cancer cells *in vitro*. More specifically, the results of the present study suggested that this complex effectively inhibited cell proliferation and induced cell apoptosis *via* the activation of the mitochondrial apoptotic signalling pathway. Taken together, these findings suggested a promising medical potential for the prepared complex in treating bacterial infections as well as cancer. The strong anticancer potential can be further delineated against other cell lines, and further *in vivo* investigations are warranted to confirm the biological effects and provide a comprehensive toxicity profile. Additional studies that will aim at enlightening the potential of this complex in suppressing cancer cell adhesion, migration and invasion are needed.

Acknowledgement

The authors thank the Doctoral School of Science and Technology at the Lebanese University for permitting access to their facilities.

Conflict of interest

The authors declare no conflict of interest.

References

1. Allardyce CS, Dyson PJ, Metal-based drugs that break the rules. *Dalton Trans.*, 2016; 45(8): 3201-3209.
2. Ghosh S, Cisplatin: The first metal based anticancer drug. *Bioorg Chem.*, 2019; 88: 102925.
3. Florea AM, Büsselberg D, Cisplatin as an anti-tumor drug: Cellular mechanisms of activity, drug resistance and induced side effects. *Cancers*, 2011; 3(1): 1351-1371.
4. Basu A, Krishnamurthy S, Cellular responses to cisplatin-induced DNA damage. *J Nucleic Acids*, 2010; 2010: 201367.
5. Dasari S, Bernard Tchounwou P, Cisplatin in cancer therapy: Molecular mechanisms of action. *Eur J Pharmacol.*, 2014; 740: 364-378.
6. Havasi A, Crișan C, Heputiu-Pater AT, Bochis OV, Cainap C, Crisan O, Balacescu O, Balacescu L, Cainap S, Platinum hypersensitivity reactions, a focus on desensitisation. *Farmacia*, 2021; 69(3): 410-418.
7. Siddik ZH, Mechanisms of action of cancer chemo-therapeutic agents: DNA-interactive alkylating agents and antitumour platinum-based drugs, The Cancer Handbook, John Wiley & Sons, Ltd, 2005.
8. Oun R, Moussa YE, Wheate NJ, The side effects of platinum-based chemotherapy drugs: a review for chemists. *Dalton Trans.*, 2018; 47(19): 6645-6653.
9. Lainé AL, Passirani C, Novel metal-based anticancer drugs: a new challenge in drug delivery. *Curr Opin Pharmacol.*, 2012; 12(4): 420-426.
10. Levina A, Mitra A, Lay PA, Recent developments in ruthenium anticancer drugs. *Metallomics*, 2009; 1(6): 458.
11. Parveen S, Recent advances in anticancer ruthenium Schiff base complexes. *Appl Organomet Chem.*, 2020; 34(8): e5687.
12. Bergamo A, Gaiddon C, Schellens JHM, Beijnen JH, Sava G, Approaching tumour therapy beyond

platinum drugs. *J Inorg Biochem.*, 2012; 106(1): 90-99.
13. Zhang S, Ding Y, Wei H, Ruthenium polypyridine complexes combined with oligonucleotides for bioanalysis: A review. *Molecules*. 2014; 19(8): 11933-11987.
14. Delaney S, Pascaly M, Bhattacharya PK, Han K, Barton JK, Oxidative damage by ruthenium complexes containing the dipyridophenazine ligand or its derivatives: A focus on intercalation. *Inorg Chem.*, 2002; 41(7): 1966-1974.
15. Cotton FA, Francis R, Sulfoxides as ligands. I. A preliminary survey of methyl sulfoxide complexes. *J Am Chem Soc.*, 1960; 82(12): 2986-2991.
16. Trotter K, Arulsamy N, Hulley E, Crystal structure of cis,fac-{N,N-bis[(pyridin-2-yl)methyl]methylamine-κ3 N,N′,N″}dichlorido(dimethyl sulfoxide-κS)ruthenium (II). *Acta Crystallogr E Crystallogr Commun.*, 2015; 71(9): m169-m170.
17. Mestroni G, Alessio E, Sava G, Pacor S, Coluccia M, Boccarelli A, Water-soluble ruthenium(III)-dimethyl sulfoxide complexes: Chemical behaviour and pharmaceutical properties. *Metal-Based Drugs*, 1994; 1(1): 41-63.
18. Hassan AS, The antibacterial activity of dimethyl sulfoxide (DMSO) with and without of some ligand complexes of the transitional metal ions of ethyl coumarin against bacteria isolate from burn and wound infection. *J Nat Sci Res.*, 2014; 4(106): 426-435.
19. Sava G, Pacor S, Mestroni G, Alessio E, Na[trans-RuCl4(DMSO)Im], a metal complex of ruthenium with antimetastatic properties. *Clin Exp Metastasis*, 1992; 10(4): 273-280.
20. Bratsos I, Jedner S, Gianferrara T, Alessio E, Ruthenium anticancer compounds: Challenges and expectations. *CHIMIA*. 2007; 61(11): 692.
21. Shukla SN, Gaur P, Kaur H, Prasad M, Mehrotra R, Srivastava RS, Synthesis, spectroscopic characterization and antibacterial sensitivity of some chloro dimethyl-sulfoxide/tetramethylenesulfoxide ruthenium(II) and ruthenium(III) complexes with 2-aminobenzothiazole. *J Coord Chem.*, 2008; 61(3): 441-449.
22. Butsch K, Gust R, Klein A, Ott I, Romanski M, Tuning the electronic properties of dppz-ligands and their palladium(ii) complexes. Dalton Trans. 2010; 39(18): 4331.
23. Hall JP, O'Sullivan K, Naseer A, Smith JA, Kelly JM, Cardin CJ, Structure determination of an intercalating ruthenium dipyridophenazine complex which kinks DNA by semiintercalation of a tetraazaphenanthrene ligand. *Proc Natl Acad Sci.*, 2011; 108(43): 17610-17614.
24. Di Pietro ML, La Ganga G, Nastasi F, Puntoriero F, Ru(II)-dppz derivatives and their interactions with DNA: Thirty years and counting. *Appl Sci.*, 2021; 11(7): 3038.
25. Horvath R, Gordon KC, Excited state vibrational spectroscopy of metal complexes of dipyrido3,2-a:2′,3′-c]phenazine. *Inorganica Chim Acta*, 2011; 374(1): 10-18.
26. Deepika N, Devi CS, Kumar YP, Reddy KL, Reddy PV, Kumar DA, Singh SS, Satyanarayana S, DNA-binding, cytotoxicity, cellular uptake, apoptosis and photocleavage studies of Ru(II) complexes. *J Photochem Photobiol B: Biol.*, 2016; 160: 142-153.
27. Li G, Sun L, Ji L, Chao H, Ruthenium(II) complexes with dppz: from molecular photoswitch to biological applications. *Dalton Trans.*, 2016; 45(34): 13261-13276.
28. Yamada M, Tanaka Y, Yoshimoto Y, Kuroda S, Shimao I, Synthesis and properties of diamino-substituted dipyrido [3,2-a: 2′,3′-c]phenazine. *Bull Chem Soc Jpn.*, 1992; 65(4): 1006-1011.
29. Evans IP, Spencer A, Wilkinson G. Dichlorotetrakis (dimethyl sulphoxide)ruthenium(II) and its use as a source material for some new ruthenium(II) complexes. *J Chem Soc Dalton Trans.*, 1973; 1973(2): 204-209.
30. Ahmed Alshwafy RY, Dahy AA, Warad I, Mahfouz RM, Synthesis and DFT calculations of new ruthenium(II) nitrosyl complexes using cis-fac-dichlorotetrakis(dimethylsulfoxide)ruthenium(II) precursor and different oximes as sources of nitrosyl ligand. *J Coord Chem.*. 2019; 72(13): 2200-2214.
31. Burke CS, Keyes TE, An efficient route to asymmetrically diconjugated tris(heteroleptic) complexes of Ru(II). *RSC Adv.*, 2016; 6(47): 40869-40877.
32. Elsayed SA, Harrypersad S, Sahyon HA, El-Magd MA, Walsby CJ, Ruthenium(II)/(III) DMSO-based complexes of 2-aminophenyl benzimidazole with *in vitro* and *in vivo* anticancer activity. *Molecules*, 2020; 25(18): 4284.
33. Singh D, Defining desirable natural product derived anticancer drug space: optimization of molecular physicochemical properties and ADMET attributes. *ADMET & DMPK.*, 2016; 4(2): 98.
34. Lipinski CA, Lead- and drug-like compounds: the rule-of-five revolution. *Drug Discov Today Technol.*, 2004; 1(4): 337-341.
35. Ertl P, Polar Surface Area, Methods and Principles in Medicinal Chemistry, Wiley, 2007; 111-126.
36. Guan L, Yang H, Cai Y, Sun L, Di P, Li W, Liu G, Tang Y, ADMET-score – a comprehensive scoring function for evaluation of chemical drug-likeness. *MedChemComm.*, 2019; 10(1): 148-157.
37. Gupta M, Lee HJ, Barden CJ, Weaver DF, The blood–brain barrier (BBB) score. *J Med Chem.*, 2019; 62(21): 9824-9836.
38. Morris GM, Lim-Wilby M, Molecular docking, Methods in Molecular Biology, Humana Press, 2008; 365-382.
39. Fan J, Fu A, Zhang L, Progress in molecular docking. *Quant Biol.*, 2019; 7(2): 83-89.
40. Andriani KF, Heinzelmann G, Caramori GF, Shedding light on the hydrolysis mechanism of cis, trans-[Ru(dmso)4Cl2] complexes and their interactions with DNA—A computational perspective. *J Phys Chem B.*, 2018; 123(2): 457-467.
41. Srishailam A, Gabra NM, Kumar YP, Reddy KL, Devi CS, Kumar DA, Singh SS, Satyanarayana S, Synthesis, characterization; DNA binding and antitumor activity of ruthenium(II) polypyridyl complexes. *J Photochem Photobiol B.*, 2014; 141: 47-58.
42. Srishailam A, Kumar YP, Venkat Reddy P, Nambigari N, Vuruputuri U, Singh SS, Satyanarayana S, Cellular uptake, cytotoxicity, apoptosis, DNA-binding, photo-cleavage and molecular docking studies of ruthenium(II)

polypyridyl complexes. *J Photochem Photobiol B.*, 2014; 132: 111-123.
43. Gaur R, Usman M, A combined experimental and theoretical investigation of ruthenium(II)-hydrazone complex with DNA: Spectroscopic, nuclease activity, topoisomerase inhibition and molecular docking. *Spectrochim Acta A Mol Biomol Spectrosc.*, 2019; 209: 100-108.
44. Gaur R, Khan RA, Tabassum S, Shah P, Siddiqi MI, Mishra L, Interaction of a ruthenium(II)–chalcone complex with double stranded DNA: Spectroscopic, molecular docking and nuclease properties. *J Photochem Photobiol A: Chem.*, 2011; 220(2-3): 145-152.
45. Yao JL, Gao X, Sun W, Shi S, Yao TM, [Ru(bpy)-2dppz-idzo]2+: a colorimetric molecular "light switch" and powerful stabilizer for G-quadruplex DNA. *Dalton Trans.*, 2013; 42(16): 5661.
46. Das D, Mondal P, Interaction of ruthenium(II) anti-tumor complexes with $d(ATATAT)_2$ and $d(GCGCGC)_2$: a theoretical study. *N J Chem.*, 2015; 39(4): 2515-2522.
47. da Silveira Carvalho JM, de Morais Batista AH, Nogueira NAP, Holanda AKM, de Sousa JR, Zampieri D, Barbosa Bezerra MJ, Barreto FS, de Moraes MO, Batista AA, Gondim ACS, de F. Paulo T, de Franca Lopes LG, Sousa EHS, A biphosphinic ruthenium complex with potent anti-bacterial and anti-cancer activity. *N J Chem.*, 2017; 41(21): 13085-13095.
48. Yang Y, Liao G, Fu C, Recent advances on octahedral polypyridyl ruthenium(II) complexes as antimicrobial agents. *Polymers*, 2018; 10(6): 650.
49. Liu X, Sun B, Kell REM, Southam HM, Butler JA, X Li, Poole RK, Keene FR, Collins JG, The antimicrobial activity of mononuclear ruthenium(II) complexes containing the dppz Ligand. *Chem Plus Chem.*, 2018; 83(7): 643-650.
50. Marquette A, Mason AJ, Bechinger B, Aggregation and membrane permeabilizing properties of designed histidine-containing cationic linear peptide antibiotics. *J Pept Sci.*, 2008; 14(4): 488-495.
51. Evans A, Kavanagh KA, Evaluation of metal-based antimicrobial compounds for the treatment of bacterial pathogens. *J Med Microbiol.*, 2021; 70(5): 001363.
52. Sun W, Boerhan R, Tian N, Feng Y, Lu J, Wang X, Zhou Q, Fluorination in enhancing photoactivated antibacterial activity of Ru(II) complexes with photo-labile ligands. *RSC Adv.*, 2020; 10(42): 25364-25369.
53. Zhang R, Chen M, Yu L, Jin Z, Anticancer activity of diphenhydramine against pancreatic cancer by stimulating cell cycle arrest, apoptosis, and modulation of PI3K/Akt/mTOR pathway. *Farmacia*, 2021; 69(5): 967-973.
54. Mahmud KM, Niloy MS, Shakil MS, Islam MA, Ruthenium complexes: An alternative to platinum drugs in colorectal cancer treatment. *Pharmaceutics*, 2021; 13(8): 1295.
55. Lee SY, Kim CY, Nam TG, Ruthenium complexes as anticancer agents: A brief history and perspectives. *Drug Des Devel Ther.*, 2020; 14: 5375-5392.
56. Muhammad N, Guo Z, Metal-based anticancer chemotherapeutic agents. *Curr Opin Chem Biol.*, 2014; 19: 144-153.
57. Mendoza-Ferri MG, Hartinger CG, Eichinger RE, Stolyarova N, Severin K, Jakupec MA, Nazarov AA, Severin K, Keppler BK, Influence of the spacer length on the *in vitro* anticancer activity of dinuclear ruthenium−arene compounds. *Organometallics*, 2008; 27(11): 2405-2407.
58. Puckett CA, Barton JK, Methods to explore cellular uptake of ruthenium complexes. *J Am Chem Soc.*, 2006; 129(1): 46-47.
59. Jenkins Y, Friedman AE, Turro NJ, Barton JK, Characterization of dipyridophenazine complexes of ruthenium(II): The light switch effect as a function of nucleic acid sequence and conformation. *Biochemistry*, 1992; 31(44): 10809-10816.
60. Huang H, Zhang P, Yu B, Chen Y, Wang J, Ji L, Chao H, Targeting nucleus DNA with a cyclometalated dipyridophenazine ruthenium(II) complex. *J Med Chem.*, 2014; 57(21): 8971-8983.
61. Mihailovic A, Vladescu I, McCauley M, Ly E, Williams MC, Spain EM, Nunez ME, Exploring the interaction of ruthenium(II) polypyridyl complexes with DNA using single-molecule techniques. *Langmuir*, 2006; 22(10): 4699-4709.
62. Mårtensson AKF, Lincoln P, Binding of Ru(terpyridine)-(pyridine)dipyridophenazine to DNA studied with polarized spectroscopy and calorimetry. *Dalton Trans.*, 2015; 44(8): 3604-3613.
63. Qian C, Wang JQ, Song CL, Wang LL, Ji LN, Chao H, The induction of mitochondria-mediated apoptosis in cancer cells by ruthenium(ii) asymmetric complexes. *Metallomics*, 2013; 5(7): 844.
64. Tan C, Wu S, Lai S, Wang M, Chen Y, Zhou L, Zhu Y, Lian W, Peng W, Ji L, Xu A, Synthesis, structures, cellular uptake and apoptosis-inducing properties of highly cytotoxic ruthenium-Norharman complexes. *Dalton Trans.*, 2011; 40(34): 8611.
65. Wang JQ, Zhang PY, Qian C, Hou XJ, Ji LN, Chao H, Mitochondria are the primary target in the induction of apoptosis by chiral ruthenium(II) polypyridyl complexes in cancer cells. *J Biol Inorg Chem.*, 2013; 19(3): 335-348.
66. Vousden KH, Activation of the p53 tumor suppressor protein. *Biochim Biophys Acta - Rev Cancer*, 2002; 1602(1): 47-59.
67. Williams AB, Schumacher B, p53 in the DNA-damage-repair process. *Cold Spring Harb Perspect Med.*, 2016; 6(5): a026070.
68. Duffy MJ, Synnott NC, O'Grady S, Crown J, Targeting p53 for the treatment of cancer. *Semin Cancer Biol.*, 2022; 79: 58-67.
69. Chipuk JE, Kuwana T, Bouchier-Hayes L, Droin NM, Newmeyer DD, Schuler M, Green DR, Direct activation of Bax by p53 mediates mitochondrial membrane permeabilization and apoptosis. *Science*, 2004; 303(5660): 1010-1014.
70. Hemann MT, Lowe SW, The p53–Bcl-2 connection. *Cell Death Differ.*, 2006; 13(8): 1256-1259.